Analysis of Bonding in Cyclopentadienyl Transition-Metal Boryl Complexes

Anthony A. Dickinson, David J. Willock,* Richard J. Calder, and Simon Aldridge*

Department of Chemistry, Cardiff University, P.O. Box 912, Park Place, Cardiff, U.K. CF10 3TB

Received June 13, 2001

Analysis of the bonding in transition-metal boryl complexes of the type $[(C_5R_5)M(CO)_2BX_2]$ has been carried out by density functional methods, to quantify the relative contributions to the metal boryl linkage from ionic and covalent interactions. Covalent (orbital) terms account for 60−70% of the overall attractive interaction between metal and boryl fragments, with σ donation from the boryl ligand overwhelmingly predominating over π back-donation even in the most favorable cases (e.g. 84.1:15.8 and 81.9:18.0 for $CpFe(CO)_2BH_2$ and $CpFe(CO)_2B(C_6F_5)_2$, respectively).

Introduction

Transition-metal boryl complexes (L_nM-BX_2) have been the subject of considerable recent research effort,[1] not least because of their implication in synthetically useful organic transformations such as the hydroboration and diboration of carbon−carbon multiple bonds.[2] More recently the involvement of cyclopentadienyl transition-metal boryl complexes in both stoichiometric[3,4] and catalytic[4,5] functionalization of alkanes and arenes has been demonstrated, notably by Hartwig.[3,5] It has been suggested that the unusual regiochemistry and activity of such systems may be due to the Lewis acidic properties of the boryl ligand, which provide favorable kinetics for the formation of boron−carbon bonds.[3e]

Such studies of reactivity have been complimented by numerous structural investigations in which the nature of the metal−boron bond has been probed by crystallographic and spectroscopic methods.[1] One of the significant questions investigated by such studies is the potential for the strongly σ donor boryl ligand also to act as a π acid by utilizing the vacant boron-based orbital of π symmetry (Chart 1). Metal boron bond lengths, together with the relative orientation of metal and boryl fragments and the IR stretching frequencies of ancillary carbonyl ligands have typically been used to probe the extent of back-bonding.[1c,3,6] In the majority of compounds studied to date it has been concluded that π interactions represent at most a relatively minor contribution to the overall metal boron bond. Such a conclusion is not unexpected, given the strongly π donating boryl substituents (e.g. X_2 = cat, *o*-$O_2C_6H_4$) and π acceptor spectator ligands (e.g. CO) commonly employed in precedented synthetic routes.[1] In such cases π donation from the metal to the ancillary carbonyl ligands and from the π donor substituents X to the boron

Chart 1. Principal Orbital Interactions for Transition Metal Boryl Complexes: σ Donor and π Acceptor Properties of the Boryl Ligand

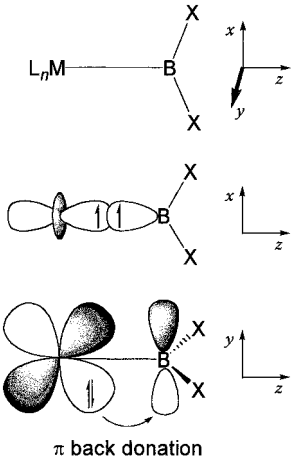

(1) (a) Wadepohl, H. *Angew. Chem., Int. Ed.* **1997**, *36*, 2441. (b) Braunschweig, H. *Angew. Chem., Int. Ed.* **1998**, *110*, 1882. (c) Irvine, G. J.; Lesley, M. J. G.; Marder, T. B.; Norman, N. C.; Rice, C. R.; Robins, E. G.; Roper, W. R.; Whittell, G. R,; Wright, L. J. *Chem. Rev.* **1998**, *98*, 2685. (d) Smith, M. R. *Prog. Inorg. Chem.* **1999**, *48*, 505.

(2) See, for example: (a) Brown, H. C.; Singaram, B. *Pure Appl. Chem.* **1987**, *59*, 879. (b) Burgess, K.; Ohlmeyer, M. J. *Chem. Rev.* **1991**, *91*, 1179. (c) Iverson, C. N.; Smith, M. R. *Organometallics* **1996**, *15*, 5155. (d) Beletskaya, I.; Pelter, A. *Tetrahedron* **1997**, *53*, 4957.

(3) (a) Hartwig, J. F.; Huber, S. *J. Am. Chem. Soc.*, **1993**, *115*, 4908. (b) Waltz, K. M.; He, X.; Muhoro, C.; Hartwig, J. F. *J. Am. Chem. Soc.* **1995**, *117*, 11357. (c) Waltz, K. F.; Hartwig, J. F. *Science* **1997**, *277*, 211. (d) Waltz, K. M.; Muhoro, C. N.; Hartwig, J. F. *Organometallics* **1999**, *18*, 3383. (e) Waltz, K. M.; Hartwig, J. F. *J. Am. Chem. Soc.* **2000**, *122*, 11358. (f) Kawamura, K.; Hartwig, J. F. *J. Am. Chem. Soc.* **2001**, *123*, 8422.

(4) Iverson, C. N.; Smith, M. R. *J. Am. Chem. Soc.* **1999**, *121*, 7696.

(5) (a) Chen, H.; Hartwig, J. F. *Angew. Chem., Int. Ed.* **1999**, *38*, 3391. (b) Chen, H.; Schlecht, S.; Semple, T. C.; Hartwig, J. F. *Science* **2000**, *287*, 1995. (c) Shimada, S.; Batsanov, A. S.; Howard, J. A. K.; Marder, T. B. *Angew. Chem., Int. Ed.* **2001**, *40*, 2168.

(6) (a) Braunschweig, H.; Ganter, B.; Koster, M.; Wagner, T. *Chem. Ber.* **1996**, *129*, 1099. (b) Braunschweig, H.; Kollann, C.; Englert, U. *Eur. J. Inorg. Chem.* **1998**, 465. (c) Braunschweig, H.; Kollann, C.; Müller, M. *Eur. J. Inorg. Chem.* **1998**, 291. (d) Braunschweig, H.; Koster, M.; Wang, R. *Inorg. Chem.* **1999**, *38*, 415. (e) Braunschweig, H.; Kollann, C.; Klinkhammer, K. W. *Eur. J. Inorg. Chem.* **1999**, 1523. (f) Yasue, T.; Kawano, Y.; Shimoi, M. *Chem. Lett.* **2000**, 58. (g) Aldridge, S.; Calder, R. J.; Dickinson, A. A.; Willock, D. J.; Steed, J. W. *Chem. Commun.* **2000**, 1377. (h) Aldridge, S.; Al-Fawaz, A.; Calder, R. J.; Dickinson, A. A.; Willock, D. J.; Light, M. L.; Hursthouse, M. B. *Chem. Commun.* **2001**, 1846.

10.1021/om0105122 CCC: $22.00
Publication on Web 02/19/2002

center are thought to predominate over MB π interaction.[7] To what extent metal−boron π back-bonding can be influenced by a wider variation in the nature of boryl substituent (X), metal (M), and ligand framework (L_n) is currently being probed by a variety of synthetic and computational approaches.

The use of DFT methods to probe the nature of the interaction between a transition-metal center and a low-coordinate group 13 ligand has received considerable recent precedent, most notably in diyl complexes of the type $L_nM{\leftarrow}EX$ (E = B, Al, Ga, In, Tl).[8−10] Evaluation of the ΔE_{elstat} and ΔE_{orb} contributions to the overall attractive metal ligand interaction has emphasized the importance of considering ionic terms in the bonding of such ligands to transition elements.[8d] However, until very recently computational studies involving boryl complexes had focused almost exclusively on reactivity and mechanism, rather than on issues of structure and bonding. The mechanisms of group 10 metal catalyzed diboration and thioboration of carbon−carbon multiple bonds, for example, have been investigated by Sakaki[11] and by Musaev and Morokuma;[12] in addition the key mechanistic steps of Rh(I)-catalyzed hydroboration of alkenes have been the subject of several computational studies.[13] Theoretical probes of structural and thermodynamic properties of metal boryl complexes have remained relatively few in number,[14] although recently Frenking et al. have reported the results of DFT studies[7] of five- and six-coordinate osmium boryl complexes originally synthesized by Roper and Wright.[15]

To shed greater light on the nature of the metal−boron interaction in boryl complexes, we have undertaken computational studies on half-sandwich boryl complexes of the type $[(C_5R_5)ML_2(BX_2)]^{n+}$ (M = Fe, Ru, n = 0; M = Co, n = 1). Such species offer several advantages over octahedral or square-pyramidal complexes as model compounds. First, the molecular orbital configuration of the $C_5R_5ML_2$ fragment is such that the relative orientation of $(C_5R_5)ML_2$ and BX_2 units can be used as a probe of π-type interactions, as has been demonstrated by Hoffmann et al. in their analysis of the pseudo-isoelectronic $CpFe(CO)_2CH_2^+$ cation.[16] In theory π-type interactions are conceivable, involving the vacant boryl-based π orbital and either the $(C_5R_5)ML_2$ HOMO of a″ symmetry (Chart 2a) or the deeper lying perpendicular HOMO-2 orbital of a′ symmetry (Chart 2b). The relative importance of these possible interactions is thought to be dependent on the steric and electronic properties of the boryl ligand.[3a] Second, comparison of calculated structural parameters with those obtained for crystallographically characterized compounds of the type $[(C_5R_5)ML_2(BX_2)]$ (M = Fe, Ru) allows some measure of the validity of the DFT method to be made.[3,6] Wide variation in Fe−B bond lengths (1.959(6)−2.195(14) Å) and in CO stretching frequencies (e.g. 2024 and 1971 cm^{-1} vs 1932 and 1869 cm^{-1}) are observed for $CpFe(CO)_2$ boryl derivatives, with the role of π interactions being described as anywhere between "modest"[3a] and nonexistent.[6c] Reproduction of structural parameters over such a breadth would therefore lend credence to the DFT method and allow an analysis of the calculated density to shed light on the origins of the observed variation.

Chart 2. Potential π Interactions between $[(C_5R_5)ML_2]$ and $[BX_2]$ Fragments: (a) Involving the Boron-Based π Orbital and the a″ Symmetry HOMO of the $[(C_5R_5)ML_2]$ Fragment; (b) Involving the Boron-Based π Orbital and the HOMO-2 of the $[(C_5R_5)ML_2]$ Fragment (of a′ Symmetry)

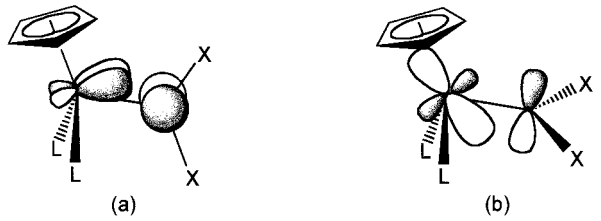

Finally, an in-depth analysis of the metal−ligand interaction might be expected to offer insight into the involvement of piano-stool cyclopentadienyl transition-metal boryl complexes in unusual (and highly useful) transformations of organic molecules. We have therefore undertaken DFT calculations on a range of such complexes in which we varied not only the boryl substituent but also the metal and ligand framework, to probe the nature of the metal−boron bond.

Results and Discussion

(i) Comparison of Calculated Structural and Spectroscopic Parameters with Experimentally Observed Values. To evaluate the accuracy of the gradient-corrected DFT method for complexes of this type, a series of calculations was carried out involving compounds for which crystallographically determined

(7) Giju, K. T.; Bickelhaupt, M.; Frenking, G. *Inorg. Chem.* **2000**, *39*, 4776.

(8) (a) Frenking, G.; Fröhlich, N. *Chem. Rev.* **2000**, *100*, 717. (b) Uddin, J.; Boehme, C.; Frenking, G. *Organometallics* **2000**, *19*, 571. (c) Boehme, C.; Uddin, J.; Frenking, G. *Coord. Chem. Rev.* **2000**, *197*, 249. (d) Uddin, J.; Frenking, G. *J. Am. Chem. Soc.* **2001**, *123*, 1683. (e) Chen, Y.; Frenking, G. *Dalton Trans.* **2001**, 434.

(9) (a) Bickelhaupt, F. M.; Radius, U.; Ehlers, A. W.; Hoffmann, R.; Baerends, E. J. *New J. Chem.* **1998**, 1. (b) Radius, U.; Bickelhaupt, F. M.; Ehlers, A. W.; Goldberg, N.; Hoffmann, R. *Inorg. Chem.* **1998**, *37*, 1080. (c) Ehlers, A. W.; Baerends, E. J.; Bickelhaupt, F. M.; Radius, U. *Chem. Eur. J.* **1999**, *4*, 210.

(10) (a) Weiss, J.; Stetzkamp, D.; Nuber, B.; Fischer, R. A.; Boehme, C.; Frenking, G. *Angew. Chem., Int. Ed.* **1997**, *36*, 70. (b) Cotton, F. A.; Feng, X. *Organometallics* **1998**, *17*, 128. (c) Boehme, C.; Frenking, G. *Chem. Eur. J.* **1999**, *5*, 2184. (d) Macdonald, C. L. B.; Cowley, A. H. *J. Am. Chem. Soc.* **1999**, *121*, 12113. (e) Linti, G.; Schnöckel, H. *Coord. Chem. Rev.* **2000**, *206−207*, 285.

(11) (a) Sakaki, S.; Kikuno, T. *Inorg. Chem.* **1997**, *36*, 226. (b) Sakaki, S.; Kai, S.; Sugimoto, M. *Organometallics* **1999**, *18*, 4825.

(12) (a) Cui, Q.; Musaev, D. G.; Morokuma, K. *Organometallics* **1997**, *16*, 1355. (b) **1998**, *17*, 742. (c) **1998**, *17*, 1383.

(13) (a) Musaev, D. G.; Mebel, A. M.; Morokuma, K. *J. Am. Chem. Soc.* **1994**, *116*, 10693. (b) Dorigo, A. E.; Schleyer, P. v. R. *Angew. Chem., Int. Ed. Engl.* **1995**, *34*, 115. (c) Musaev, D. G.; Matsubara, T.; Mabal, A. M.; Koga, N.; Morokuma, K. *Pure Appl. Chem.* **1995**, *67*, 257. (d) Widauer, C.; Grützmacher, H.; Ziegler, T. *Organometallics* **2000**, *19*, 2097.

(14) (a) Rablen, P. R.; Hartwig, J. F.; Nolan, S. P. *J. Am. Chem. Soc.* **1994**, *116*, 4121. (b) Rablen, P. R.; Hartwig, J. F. *J. Am. Chem. Soc.* **1996**, *118*, 4648. (c) Wagner, M.; Hommes, N. J. R. v. E.; Nöth, H.; Schleyer, P. v. R. *Inorg. Chem.* **1995**, *34*, 607. (d) Musaev, D. G.; Morokuma, K. *J. Phys. Chem.* **1996**, *100*, 6509.

(15) (a) Irvine, G. J.; Roper, W. R.; Wright, L. J. *Organometallics* **1997**, *17*, 4869. (b) Rickard, C. E. F.; Roper, W. R.; Williamson, A.; Wright, L. J. *Organometallics* **1998**, *17*, 4869. (c) Rickard, C. E. F.; Roper, W. R.; Williamson, A.; Wright, L. J. *Angew. Chem., Int. Ed.* **1999**, *38*, 1110. (d) Irvine, G. J.; Rickard, C. E. F.; Roper, W. R.; Williamson, A.; Wright, L. J. *Angew. Chem., Int. Ed.* **2000**, *39*, 948. (e) Rickard, C. E. F.; Roper, W. R.; Williamson, A.; Wright, L. J. *Organometallics* **2000**, *19*, 4344.

(16) Schilling, B. E. R.; Hoffmann, R.; Lichtenberger, D. *J. Am. Chem. Soc.* **1979**, *101*, 585. (b) Wilker, C. N.; Hoffmann, R.; Eisenstein, O. *Nouv. J. Chem.* **1983**, *7*, 535.

Table 1. Calculated (in Italics) and Crystallographically Determined Structural Parameters for Iron−Boryl Complexes 1−8

	distance (Å)				angle (deg)		
	Fe−B	Fe−Cp centroid	mean Fe−L	mean B−X	L−Fe−L	X−B−X	ϑ[a]
1	1.959(6)	1.716(1)	1.731(6)	1.411(7)	92.9(3)	108.0(5)	7.9
	2.009	*1.809*	*1.765*	*1.420*	*94.6*	*109.4*	*1.4*
2							
	2.002	*1.772*	*1.767*	*1.414*	*94.6*	*108.3*	*2.7*
3	1.980(2)	1.72(1)	1.746(3)	1.407(3)	96.3(1)	108.8(2)	26.7
	2.027	*1.802*	*1.767*	*1.420*	*95.3*	*107.6*	*28.1*
4	1.971(2)	1.721(2)	1.755(2)	1.406(2)	94.0(8)	109.2(1)	82.2(1)
	2.015	*1.804*	*1.773*	*1.415*	*94.2*	*109.7*	*83.4*
5	2.034(3)	1.729(1)	1.748(3)	1.577(3)	90.8(1)	116.6(2)	75
	2.107	*1.824*	*1.762*	*1.582*	*89.0*	*118.2*	*66.8*
6[b]	2.027(5)	1.735(1)	1.746	1.377(6) N 1.834(5) Cl	93.6	112.0(3)	87.4
	2.058	*1.823*	*1.763*	*1.409 N* *1.855 Cl*	*94.3*	*111.7*	*75.2*
7[c]	2.195(14)	*d*	*d*	1.924(15) P	*d*	*d*	*e*
	2.215	*1.820*	*1.758*	*1.211 H* *1.971 P*	*94.7*	*114.7*	*e*
8[f]	1.965(5)	1.734(4)	1.755(4)	1.596(5)	94.5(2)	111.5(3)	28.2(3)
	2.006	*1.823*	*1.776*	*1.597*	*93.3*	*114.0*	*40.5*

[a] The angle ϑ is defined in Chart 3. [b] Calculations employed the simplification of using the $B(Cl)NH_2$ ligand, rather than $B(Cl)NMe_2$. [c] Calculations employed the simplified ligands PH_3 and C_5Me_5, rather than PMe_3 and C_5Me_4Et. [d] Data not available. [e] Not applicable. [f] Crystallographically determined values for **8** are the mean values for the two independent molecules within the asymmetric unit.

structural data are available. The range of compounds investigated allows for wide variation in the nature of the Fe−B bond, by altering (i) the π donor capacity of the boryl substituent, X (e.g. BX_2 = Bcat (**1**, **3**), BPh_2 (**5**), $B(Cl)NH_2$ (**6**), and $B(C_6F_5)_2$ (**8**)), (ii) the electronic and steric requirements of the cyclopentadienyl ligand (e.g. Cp, C_5H_5 (**1**, **4**, **5**) and Cp*, C_5Me_5 (**3**, **6**, **7**)), (iii) the mode of coordination of the boryl ligand (e.g. terminal Bcat (**1**, **3**) vs bridging $BO_2C_6H_2O_2B$ (**4**)), and (iv) the availability of the boryl-based π orbital for back-bonding (e.g. using the base-stabilized boryl **7**, incorporating a four-coordinate boron center). Satisfactory agreement with experimentally determined structural parameters and reproduction of observed trends over such a range of compounds would then provide a strong indication of the reliability of the DFT method. The results of these calculations are reproduced in Tables 1 and 2 and Figure 1, which compare calculated and experimentally observed bond lengths and angles. The agreement between theoretically predicted and experimentally observed geometries is generally very good. The calculated Fe−B distances for all complexes are typically 2−3% greater than those obtained crystallographically; such an overestimation of bond lengths involving heavier atoms by DFT is well precedented.[17] Frenking et al., for example, in their recent study of osmium boryl complexes found a similar overestimation of OsB distances (e.g. 2.046 Å (exptl) vs 2.104 Å (calcd) for the five-coordinate species $(R_3P)_2OsCl(CO)B(OH)_2$), a discrepancy which has been attributed to solid-state effects which lead to the shortening of donor−acceptor bonds.[7] It is interesting to note, however, that the differences between observed and calculated FeB distances are reasonably constant and, therefore, that the DFT method reproduces well-observed *trends* in this parameter. In particular, the shorter Fe−B lengths found for boryl ligands bearing oxygen substituents and the somewhat longer distances found for BPh_2, $B(Cl)NH_2$, and especially $BH_2{\cdot}PR_3$ ligands are reflected in the corresponding calculated values.

Chart 3. Definition of the Angle ϑ between the C_5R_5 Centroid−Fe−B and BX_2 Planes

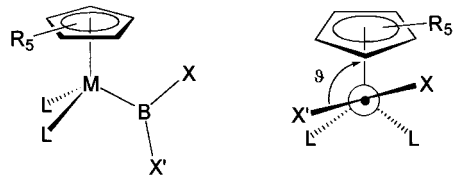

The geometries of $Fe(CO)_2$ and BX_2 units have been extremely well reproduced computationally, and there is also reasonable agreement between observed and calculated values for ϑ, defined in Chart 3 as the angle between the Cp centroid−Fe−B and BX_2 planes. As has been noted previously,[3a] the magnitude of ϑ is dependent on several factors, notably the π acceptor capacity and steric requirements of the BX_2 ligand. In fact, rotation about the Fe−B bond represents motion across a very shallow potential energy surface (vide infra), with the difference in energy for several rotamers often being very small. It is reassuring, therefore, that despite such small energy differences, the calculations do reproduce with reasonable accuracy the experimentally observed torsion angles. In particular, the contrasting near-coplanar (7.9 and 26.7°) and near-perpendicular (82.2°) geometries determined experimentally for the superficially similar complexes of terminal Bcat (**1** and **3**)[3a,d] and bridging $BO_2C_6H_2O_2B$ ligands (**4**)[6g] are reproduced well by these calculations (1.4, 28.1, and 83.4°, respectively).

Finally, calculated parameters are also included for complex **2**, featuring the "cut-down" catecholboryl ligand $-BO_2C_2H_2$. Differences between data calculated for this simplified ligand system and the full catechol system

(17) See, for example: McCullough, E. A., Jr.; Aprà, E.; Nichols, J. *J. Phys. Chem. A* **1997**, *101*, 2502.

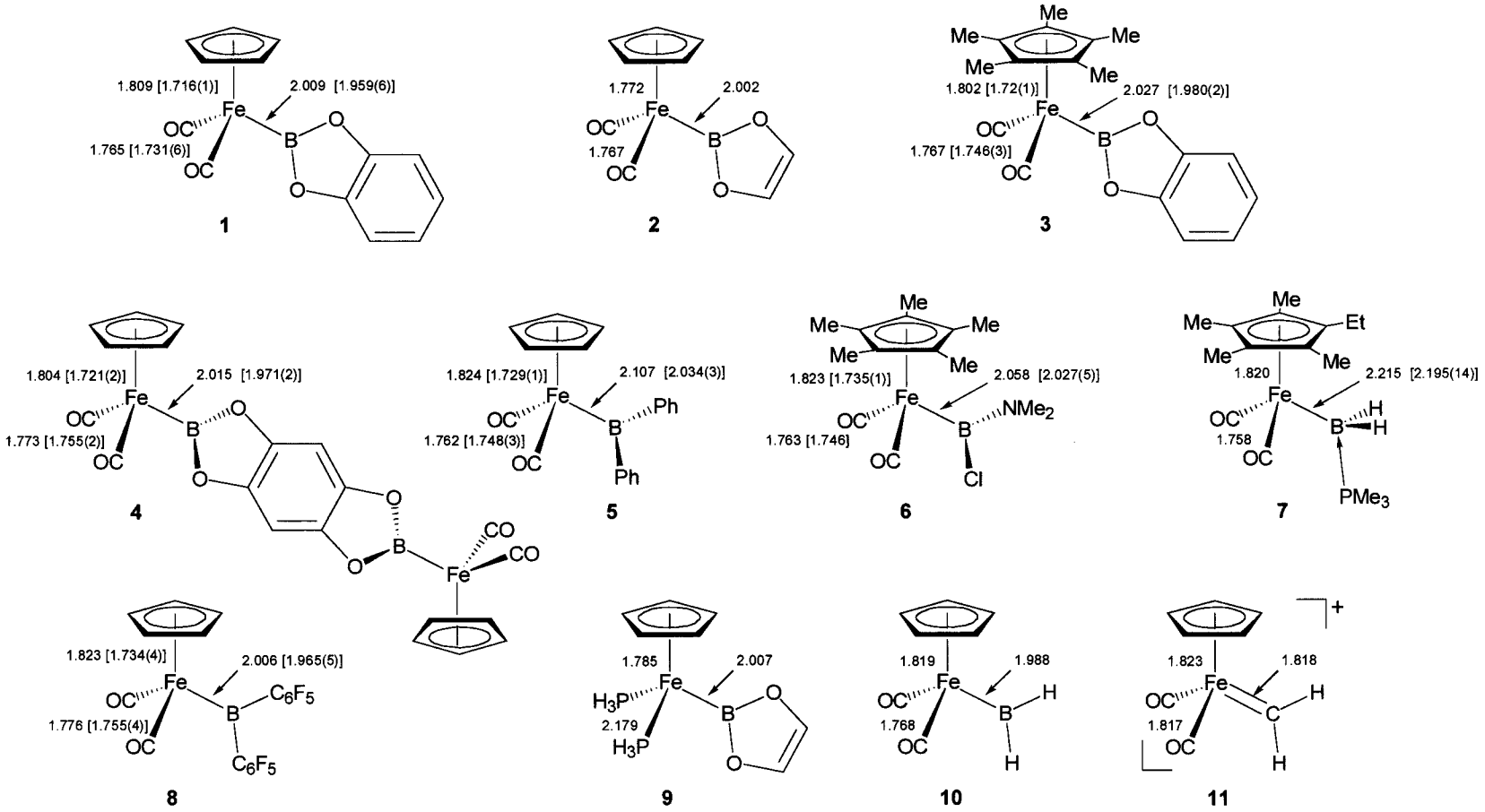

Figure 1. Calculated and crystallographically determined [in parentheses] bond lengths (Å) for compounds **1**−**11**. Calculated structures for complexes **6** and **7** employed the simplifications of using $B(NH_2)Cl$ rather than $B(NMe_2)Cl$ (for **6**) and C_5Me_5 and PH_3 rather than C_5Me_4Et and PMe_3 (for **7**). Crystallographically determined values for **8** are the mean values for the two independent molecules within the asymmetric unit.

Table 2. Complexes of the Type $[(C_5R_5)ML_2BX_2]^{n+}$ Investigated by DFT in This Study

compd	M	*n*	L	R	X	X′
1	Fe	0	CO	H	cat	
2	Fe	0	CO	H	$O_2C_2H_2$	
3	Fe	0	CO	Me	cat	
4	Fe	0	CO	H	$O_2C_6H_2O_2BFe(CO)_2Cp$	
5	Fe	0	CO	H	Ph	Ph
6	Fe	0	CO	Me	Cl	NH_2
7[a]	Fe	0	CO	Me	H	H
8	Fe	0	CO	H	C_6F_5	C_6F_5
9	Fe	0	PH_3	H	$O_2C_2H_2$	
10	Fe	0	CO	H	H	H
12	Fe	0	CO	H	F	F
13	Fe	0	CO	H	Cl	Cl
14	Fe	0	CO	H	$O_2C_6Cl_4$ (catCl_4)	
15	Fe	0	CO	Me	$O_2C_2H_2$	
16	Fe	0	PH_3	H	H	H
17	Fe	0	PH_3	H	F	F
18	Fe	0	PH_3	H	Cl	Cl
19	Co	1	CO	H	$O_2C_2H_2$	
20	Ru	0	CO	H	$O_2C_2H_2$	

[a] Contains the PH_3 ligand coordinated at the boron center.

Table 3. Effect of Variation in Level of Theory and Basis Set on the Fe−B Bond Length (Å) Calculated for Model Compound 2[a]

	STO-3G	LANL2DZ	6-311G(d)	6-31+G(d)	6-311++G(d)
BLYP	1.958	1.992	2.009	2.011	2.004
B3LYP	1.966	1.975	1.992	2.001	2.002

[a] A distance of 2.002 Å was calculated from BLYP(ADF) using basis set IV.

proved to be very small (less than 2%), such that the reduced ligand was employed in computationally more demanding analyses, including the calculation of energetic profiles for rotation about the Fe−B bond. A similar simplification was employed by Frenking et al. in their recent analysis of osmium boryl complexes.[7]

In an attempt to gauge the effect of different levels of computational theory and of different basis sets on the accuracy of calculated structural parameters, the geometry of complex **2** was optimized using both BLYP and B3LYP levels of theory and five different basis sets (from a simple STO-3G basis to 6-311++G(d)). The results of this analysis are outlined in Table 3, which highlights changes in the Fe−B bond length. As expected, the B3LYP hybrid functional leads to shorter calculated Fe−B bond lengths (and to values which are closer to the experimentally observed value of 1.959 Å for the full catecholboryl complex), although the improvement over the values calculated using BLYP are always less than 2%. Perversely, the best estimates for the Fe−B distance are obtained with the smallest basis sets. However, the convergence of this bond length with increased size of basis set suggests that this is most probably due to a fortuitous cancellation of errors between the DFT method and basis set inadequacies. Furthermore, the fact that our standard ADF/STO calculation for **2** gives a bond length similar to that obtained using the higher quality Gaussian basis set G-311++G(d) (B3LYP) gives us additional confidence in the accuracy of our method. Since we wish to analyze the model density for bonding character, we must consider results from this level of basis set to ensure our comparison of different boryl systems is based on accurate model densities. At this level of theory the range of compounds given in Figure 1 have experimental Fe−B bond lengths spread over an interval of 0.236 Å and we find a systematic overestimate of around 0.05 Å. This level of accuracy gives us confidence in interpreting the bonding character of the metal boryl systems presented in the following sections.

(ii) Analysis of Electronic Structure and Bonding in $CpFe(CO)_2BO_2C_2H_2$, $CpFe(PH_3)_2BO_2C_2H_2$, $CpFe(CO)_2BH_2$, and $CpFe(CO)_2CH_2^+$. To gain insight into the electronic structure and bonding of half-sandwich iron boryl complexes, a more in-depth analysis was undertaken for the model complexes $CpFe(CO)_2BO_2C_2H_2$ (**2**) and $CpFe(PH_3)_2BO_2C_2H_2$ (**9**), as well as for the isoelectronic pair of hydrogen-substituted species $CpFe(CO)_2BH_2$ (**10**) and $CpFe(CO)_2CH_2^+$ (**11**). The first two complexes serve as models for the molecules $CpFe(CO)_2$Bcat and $CpFe(PMe_3)_2$Bcat synthesized by Hartwig,[3a,d] whereas the BH_2 complex **10**, although likely to represent a significant synthetic challenge, offers an instructive comparison with the isoelectronic alkylidene **11**, which by analogy with related complexes (e.g. $CpFe(CO)_2(CCl_2)^+$ [18] and $CpFe(CO)_2(C_7H_6)^+$ [19]) would be expected to contain an Fe−C double bond. Although the overall bond order and degree of π interaction will intuitively be smaller for boryl systems compared to isoelectronic cationic alkylidenes, analysis of complex **11** provides a baseline against which results for various boryl complexes can be compared. Our analysis of the geometric data, molecular orbital composition, electron density difference maps, Fe−B rotational barriers, bond order, energy partitioning analysis, and bonding density decomposition allow us to make several conclusions about the nature of the metal−ligand interaction in such complexes.

An initial survey of the geometric data for **2** and **11** (Figure 1) reveals not unexpectedly that, for the model catecholboryl ligand $BO_2C_2H_2$, the Fe−B bond order is likely to be somewhat less than the Fe−C bond order found in the alkylidene complex **11**. The calculated Fe−C distance (1.818 Å) is significantly shorter than the sum of the covalent radii for Fe and C (2.02 Å),[20] but this is not reproduced to the same degree in the calculated Fe−B distance for **2**. The calculated Fe−B distance for **2** is 2.002 Å, compared with 2.15 Å for the sum of the covalent radii of Fe and B,[20] or 2.105 Å for the sum of half of the Fe−Fe distance in $[CpFe(CO)_2]_2$ and half of the B−B distance in B_2cat_2.[21,22] Electron density difference maps for **2** and **11** (reproduced in the Supporting Information) reveal an elliptical shift in electron density on Fe−C bond formation, consistent with a significant π contribution to bonding for **11**. Conversely, the analogous plot for **2** reveals a near-circular cross-section to the shift in electron density on Fe−B bond formation, consistent with a predominantly σ-type interaction.

A more rigorous analysis of the nature of the Fe−B and Fe−C bonds can be obtained by examination of the

(18) Crespin, A. M.; Shriver, D. F. *Organometallics* **1985**, *4*, 1830.
(19) Riley, P. E.; Davis, R. E.; Allison, N. T.; Jones, W. M. *J. Am. Chem. Soc.* **1980**, *102*, 2458.
(20) Huheey, J. E.; Keiter, E. A.; Keiter, R. L. *Inorganic Chemistry: Principles of Structure and Reactivity*; Harper Collins: New York, 1993.
(21) Bryan, R. F.; Greene, P. T.; Newlands, M. J.; Field, D. S. *J. Chem. Soc. A* **1970**, 3068.
(22) Nguyen, P.; Lesley, G.; Taylor, N. J.; Marder, T. B.; Picket, N. L.; Clegg, W.; Elsegood, M. R. J.; Norman, N. C. *Inorg. Chem.* **1994**, *33*, 4623.

various atomic orbital contributions to the molecular orbitals of molecules **2** and **9**−**11** (important molecular orbitals for complexes **2** and **11** are represented in Figure 2; a fuller listing for all four complexes can be found in the Supporting Information). Although the one-electron orbitals in a DFT model are formally only a route to construction of the density, the use of atomic orbitals as basis sets leads to orbitals with the same shape, symmetry, and energetic ordering as wave function based calculations.[23] For the lowest energy conformation of the alkylidene molecule **11** (with a near-coplanar, $\vartheta = 0.1°$, arrangement of the Cp centroid−Fe−C and CH_2 planes), examination of the molecular orbitals reveals that the Fe−C interaction is characterized by a strong σ bond (HOMO-5, featuring significant in-phase contributions from Fe $3d_{z^2}$ and C $2p_z$ orbitals, LUMO+2 being the corresponding unoccupied antibonding combination). This is supplemented by a π type interaction predominantly featuring the Fe $3d_{yz}$ and C $2p_y$ orbitals (the bonding combination being HOMO-2 and the antibonding being the LUMO). The remaining occupied frontier orbitals above the σ bonding HOMO-5 (i.e. the HOMO, HOMO-1, HOMO-3, and HOMO-4) are mainly Fe 3d in nature. Such an analysis is in good agreement with that reported by Hoffmann and co-workers in 1979.[16a]

A corresponding molecular orbital analysis has also been made for the boryl complexes **2**, **9,** and **10** (see Figure 2). An instructive comparison can be made between the MO descriptions of bonding in the isoelectronic pair of molecules $CpFe(CO)_2BH_2$ (**10**) and $CpFe(CO)_2CH_2^+$ (**11**). σ bonding between iron and boryl fragments in **10** is represented by HOMO-3, which, like its counterpart for alkylidene **11**, contains significant contributions from Fe $3d_{z^2}$ and B $2p_z$. The differences between the bonding in these molecules revolve around the use of the Fe $3d_{yz}$ orbital. In the case of the alkylidene **11** this atomic orbital plays a major role in the HOMO-4 bonding molecular orbital between Fe and the cyclopentadienyl ligand (HOMO-4: 31.8% Fe $3d_{yz}$) and also in π bonding to the alkylidene fragment (HOMO-2 contains 22.4% Fe $3d_{yz}$). These two orbitals are separated by some 0.6 eV. In boryl complex **10** the Fe $3d_{yz}$ orbital is also involved in π type interactions with both cyclopentadienyl and boryl ligands, as evidenced by significant contributions to HOMO-1 and HOMO-2. In contrast to the situation in **11**, however, these two orbitals are nearly degenerate ($\Delta E = 0.02$ eV) and *both* contain significant Fe−Cp and Fe−B π bonding character. Most significant, however, is the observation that the *total* contribution of the B $2p_y$ orbital to both of these MOs (7.8%) is markedly less than the contribution of the C $2p_y$ orbital to the analogous MO in molecule **11** (21.0% to HOMO-2). Likewise, the MOs for **10** which represent the Fe−B π* antibonding interaction (LUMO and LUMO+2) contain smaller amounts of Fe $3d_{yz}$ character (19.4% in total) than does the corresponding FeC π* MO in **11** (23.5% Fe $3d_{yz}$ in the LUMO). In addition, the energy difference between orbitals of π and π* character (4.1 eV) is somewhat greater than in the case of the alkylidene (3.2 eV).

As expected, these observations confirm that the π interaction between $[CpFe(CO)_2]$ and alkylidene/boryl fragments is weaker in the case of boron (a conclusion also reached on the basis of bond partition analysis (vide infra)). This is primarily due to the higher energy of the $2p_y$ orbital required for π bonding in the case of the boryl ligand (3.65 eV for the BH_2^- fragment, compared to −4.80 eV for CH_2). This results in a larger energy difference between the Fe $3d_{yz}$ and E $2p_y$ orbitals in the case of E = B and, therefore, in less efficient orbital mixing (as reflected by smaller B $2p_y$ contributions to MOs with Fe−B π bonding character and smaller Fe $3d_{yz}$ contributions to MOs with Fe−B π* character).

The significance of π contributions to Fe−B bonding can be seen to further diminish on replacement of the H substituents of the boryl ligand by π donor oxygen-based substituents: for example, in $BO_2C_2H_2$. For this ligand in complex **2** the expected strong σ interaction between $CpFe(CO)_2$ and $BO_2C_2H_2$ fragments is represented by HOMO-4, which again features significant contributions from Fe $3d_{z^2}$ and B $2p_z$ and 2s orbitals (see Figure 2). However, the HOMO-2 orbital which, as in the case of alkylidene **11**, represents the predominant Fe−B π bonding interaction, notably has a much smaller contribution from B $2p_y$ (5.3%) than do the corresponding MOs for **10** (7.8% B $2p_y$) and **11** (21.0% C $2p_y$). Furthermore, it is possible to identify orbitals at ca. −8.0 and +0.9 eV (LUMO+12) which have significant character as (filled) B−O π and (unfilled) B−O π* MOs, respectively. The contribution of Fe $3d_{yz}$ to either of these orbitals is negligible. The DFT-calculated molecular orbital analysis for compound **2** is therefore consistent with a boryl ligand which acts as a strong σ donor but which interacts to a much smaller degree with Fe-based orbitals of π symmetry due to competing O−B π interaction. On examination of the molecular orbital makeup for the fragment $BO_2C_2H_2^-$, in effect the available π symmetry orbital at boron has been shifted to much higher energy (5.41 vs 3.65 eV for BH_2^-), as it is effectively a B−O π* orbital (the filled orbital with B−O bonding character being found at −5.20 eV). A simplified description of the π type interactions between metal and boryl/alkylidene fragments in molecules **2**, **10**, and **11** is reproduced in Figure 3 and is fully consistent with the calculated orbital energies for the CH_2, BH_2^-, and $BO_2C_2H_2^-$ fragments, the vacant orbital of appropriate (π) symmetry on the boryl/alkylidene fragment being found at −4.80, 3.65, and 5.41 eV, respectively (the lower energy filled BO π bonding MO for the $BO_2C_2H_2^-$ fragment has an energy of −5.20 eV).

We have also attempted to quantify the σ and π contributions to covalent bonding by using the orbital symmetry partitioning method described in the Computational Section and which has been tested for a range of model compounds (details of the calculations and data for C_2H_n ($n = 2, 4, 6$), N_2, and CO are included in the Supporting Information). The results of this analysis are included in Table 4 and further emphasize the relatively minor role of π interactions for transition-metal boryl complexes demonstrated by the preceding MO analysis. The model catechol species **2**, for example, is characterized by a 87.6:12.3 breakdown of σ and π covalent character to the Fe−B bond. The relative importance of π bonding increases, as might be expected, on replacement of the oxygen-derived boryl substituents (for **2**) by non π donor hydrogen atoms (for **10**) and by

(23) Stowasser, R.; Hoffmann, R. *J. Am. Chem. Soc.* **1999**, *121*, 3414.

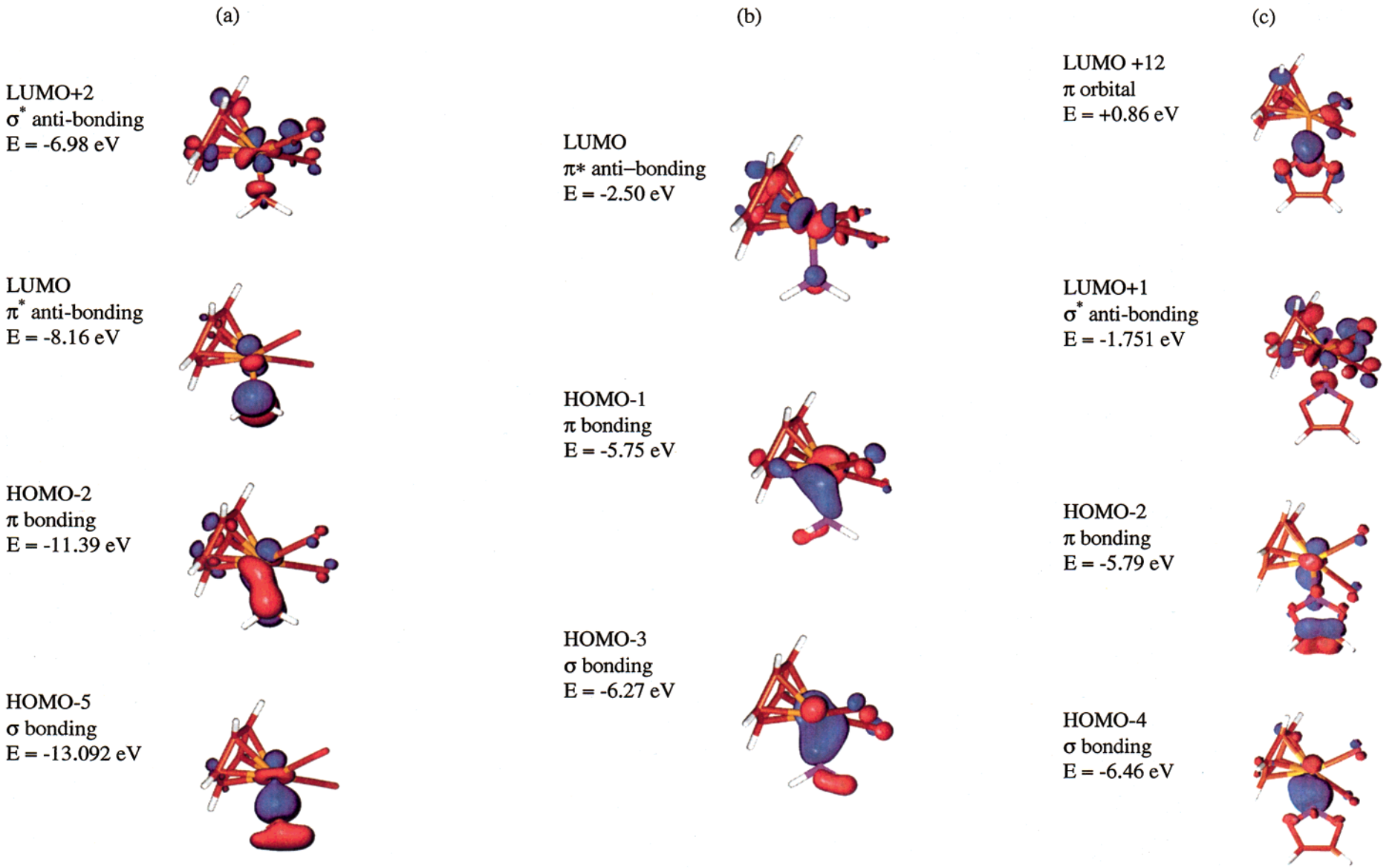

Figure 2. Plots of important molecular orbitals (a) for cationic alkylidene **11**, (b) for boryl complex **10**, and (c) for boryl complex **2**. All orbitals are plotted using the same Molden contour level of 0.07 e $Å^{-3}$. Note that the Fe−B and Fe−C bonds are oriented along the *z* axis for ease of interpretation of MOs.

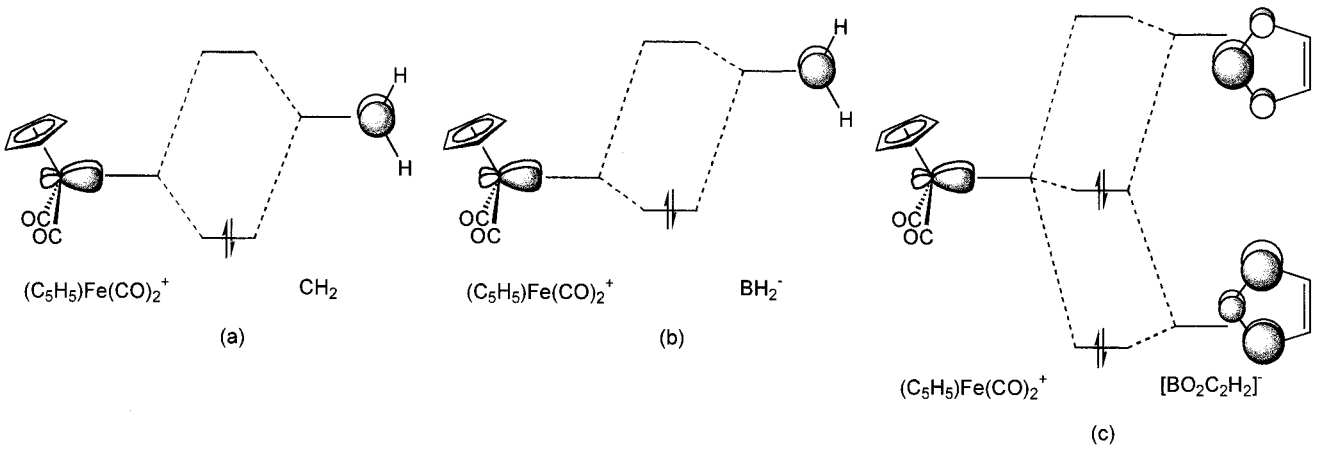

Figure 3. Simplified π orbital interaction diagram for compounds (a) **11**, (b) **10**, and (c) **2**.

Table 4. Analysis of Bonding in Complexes 1−20

compd	calcd r(M−E)/Å[a]	breakdown of orbital contribn to bond/% σ	π	Mayer bond order	BDE (D_o)/ kcal mol^{-1}	ΔE_{elstat}[b]/ kcal mol^{-1}	ΔE_{orb}[b]/ kcal mol^{-1}	ΔE_{Pauli}[b]/ kcal mol^{-1}	$\Delta E_{elstat}/\Delta E_{orb}$
1	2.009	89.2	10.7	0.957	66.1	−110.5	−224.5	247.6	0.49
2	2.002	87.6	12.3	0.920	64.8	−93.0	−201.3	208.8	0.46
3	2.027	87.0	12.9	0.856	65.2	−112.1	−225.7	250.0	0.50
4	2.015	87.2	12.1	0.935	65.2	−115.5	−227.6	256.5	0.51
5	2.107	90.4	9.5	0.888	45.5	−60.8	−322.4	107.5	0.19
6	2.058	86.9	13.0	0.904	55.3	−118.4	−204.6	240.8	0.58
7	2.215	97.2	2.9	0.694	40.0	−85.9	−157.3	173.6	0.55
8	2.006	81.9	18.0	0.999	53.6	−112.9	−194.2	228.0	0.58
9	2.007	85.0	14.8	1.016	68.5	−121.8	−233.2	261.7	0.52
10	1.988	84.1	15.8	0.995	66.8	−136.2	−239.6	285.6	0.57
11	1.818	63.8	36.3	0.995	80.0	−179.3	−121.1	201.9	1.48
12	2.010	94.0	6.0	0.980	65.9	−110.4	−224.5	244.1	0.49
13	2.008	82.1	17.8	1.020	58.1	−116.3	−226.8	250.3	0.51
14	1.995	86.1	13.8	0.961	67.3	−107.9	−226.4	242.7	0.48
15	2.020	86.5	13.4	0.923	65.1	−111.3	−224.4	249.0	0.50
16	1.970	82.1	17.7	1.173	70.0	−145.3	−243.0	291.6	0.60
17	2.024	87.5	12.3	1.165	69.2	−106.1	−203.1	211.2	0.52
18	1.972	77.2	22.6	1.195	64.4	−128.2	−231.8	265.0	0.55
19	1.993	95.7	4.2	0.766	66.1	−103.5	−197.9	214.0	0.52
20	2.112	79.4	20.4	0.939	76.9	−130.9	−234.0	272.1	0.56

[a] E = B for complexes **1**−**10** and **12**−**20**; E = C for complex **11**. [b] ΔE_{elstat}, ΔE_{orb}, and ΔE_{Pauli} are respectively the contributions to the instantaneous interaction energy (between metal and boryl fragments) due to electrostatic attraction, orbital interaction, and Pauli repulsion ($\Delta E_{int} = \Delta E_{elstat} + \Delta E_{orb} + \Delta E_{Pauli}$). The ratio $\Delta E_{elstat}/\Delta E_{orb}$ gives information about the relative importance of ionic and covalent contributions to the metal−boron bond.[8d]

the employment of less π acidic ligands such as phosphines at the metal center (for **9**). In none of the compounds examined during the course of this study, however, does the significance of π bonding (as calculated by this partition method) approach that observed for the alkylidene complex **11** (for which a 63.8:36.2 σ:π breakdown is calculated). Finally, given the 2−3% overestimate in calculated metal−boron bond lengths found in this and other DFT studies,[7] together with the likely sensitivity of the π bonding contribution to changes in the metal−boron length, we sought to investigate whether fixing the M−B distance at the crystallographically determined value would significantly affect the nature of the metal−boron bond. To this end, the Fe−B distance for compound **1** was fixed at the experimental value of 1.959 Å,[3a] and the remainder of the structure was allowed to relax. This approach results in only marginally higher Mayer bond order (0.974 vs 0.957) and π contribution to bonding (12.3 vs 10.7%) when compared to the minimum energy calculated structure.

Traditionally, in the absence of substituent steric effects the size of the energy barrier associated with rotation about a particular bond has been related to the degree of noncylindrical (i.e. π or δ) bonding character. In the case of the systems investigated here, analysis of the energetic profile for rotation about the Fe−B bond is complicated by the existence of two mutually perpendicular metal-based orbitals with which the boryl ligand can engage in π bonding. Nevertheless, investigation of the energy profile for rotation about the Fe−B bond for compounds **2** and **9** offers an alternative method to probe the nature of the metal−ligand interaction. With a coplanar ($\vartheta = 0°$) orientation of the Cp centroid−Fe−B and BX_2 planes as a starting point, a rotational profile was calculated for the reduced catecholboryl derivative **2** by varying the interplanar angle ϑ in incremental steps of 9° and allowing geometric relaxations at each point under this single constraint of fixed interplane angle. The results of this analysis are illustrated in Figure 4.

Several features are apparent from the rotational profile. First, two minima are observed (at ca. 10 and 80°) in the plot of total energy vs ϑ. The relative energies of these two conformers are very similar indeed ($\Delta E <$ 0.025 kcal mol^{-1}), and the π contributions to bonding

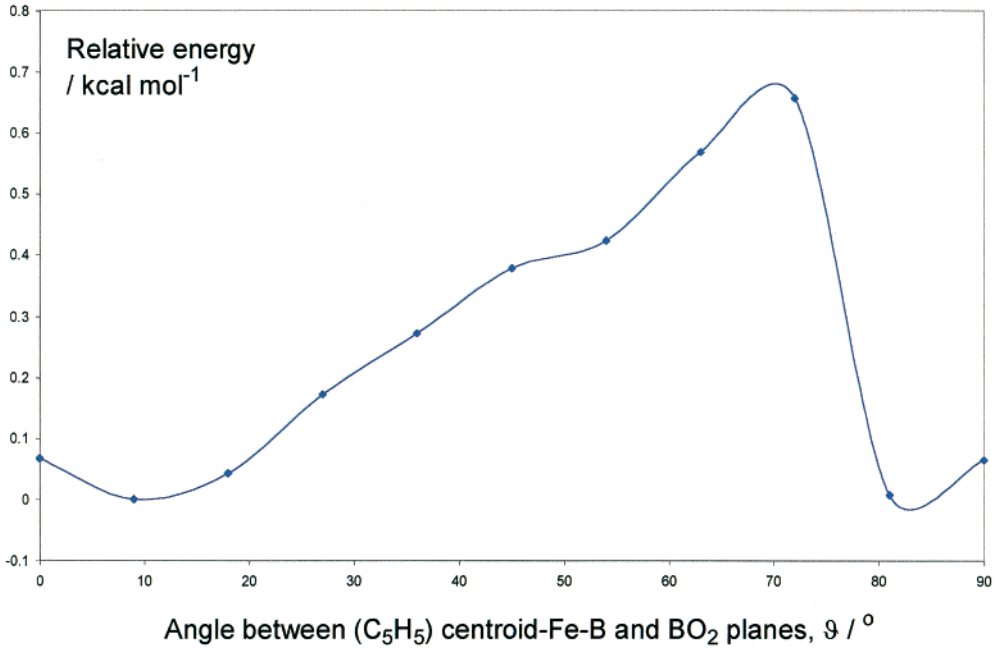

Figure 4. Energetic profile for rotation about the Fe−B bond in compound **2**.

are very similar in each case (12.2 and 13.8%, respectively). This reflects the fact that π bonding is possible involving the vacant boryl-based π orbital and either the $CpFe(CO)_2$ HOMO of a″ symmetry (to which Fe $3d_{yz}$ is a significant contributor) or the deeper lying perpendicular HOMO-2 orbital of a′ symmetry (which features Fe $3d_{xz}$) (see Chart 2).[16a] The extent of π bonding appears to be similar in each case, and with σ bonding being axially symmetric, near-identical energies are therefore calculated for the two conformers. It is interesting therefore that crystallographic studies reveal that the superficially similar terminal and bridging boryl complexes **1** and **4** exhibit very different values of ϑ (7.9[3a] and 82.2°,[6g] respectively). Given the relatively low barrier to rotation about the Fe−B bond and the similar energies calculated for near-perpendicular ($\vartheta \approx 80°$) and near-coplanar ($\vartheta \approx 10°$) conformers of the model compound **2**, it seems likely that the adoption of either conformation in the solid state could well be determined by the energetics of molecular packing in the crystalline state, rather than by the electronic nature of the metal−ligand bond.

The size of the barrier to rotation about the Fe−B bond in this case cannot be used to give a true indication of the strength of Fe−B π bonding. A number of factors, notably the existence of two mutually perpendicular sets of appropriate symmetry orbitals on the metal fragment, complicate the interpretation of the rotational profiles in this case.[24] It can be noted, however, that the magnitude of the calculated barriers for **2** (ca. 1 kcal mol^{-1}) and the phosphine derivative $CpFe(PH_3)_2BO_2C_2H_2$ (**9**) (ca. 2 kcal mol^{-1}) are significantly less than that measured by Brookhart and Studabaker for the alkylidene $[CpFe(Ph_2PCH_2CH_2PPh_2)CH_2]^+$ (10.8 kcal mol^{-1} [25]).

(24) Dickinson, A. A.; Willock, D. J.; Aldridge, S. Manuscript in preparation.
(25) Studabaker, W. B.; Brookhart, M. *J. Organomet. Chem.* **1986**, *310*, C39.

(iii) Effects of Variation in Metal (M), Ligand Framework (L_n), and Boryl Substituent (X). In an attempt to determine how the nature of the metal−boron bond changes with wider variation in its steric and electronic environment, we have undertaken DFT studies for compounds **1**−**20**, the results of which are listed in Table 4. These model compounds encompass variation in metal (Fe, Ru, Co), ligand (CO, PH_3, Cp, Cp*), and boryl substituent (encompassing H, F, Cl, Ph, C_6F_5, and NH_2 substituents as well as catechol-based derivatives) and have been analyzed not only in terms of bond lengths and bond orders but also in terms of homolytic bond dissociation energies (D_o, BDEs). In addition, we have partitioned the instantaneous interaction energy (ΔE_{int}) between metal and boryl fragments into attractive terms relating to electrostatic (ΔE_{elstat}) and orbital (ΔE_{orb}) components and repulsive Pauli terms (ΔE_{Pauli}; $\Delta E_{int} = \Delta E_{elstat} + \Delta E_{orb} + \Delta E_{Pauli}$) in a manner analogous to that used by Uddin and Frenking in their recent analysis of group 13 diyl complexes of iron and nickel.[8d] In this way the relative importance of electrostatic and covalent contributions to the M−B bond can also be evaluated (through the ratio $\Delta E_{elstat}/\Delta E_{orb}$). Finally, the relative importance of σ and π symmetry covalent interactions have been assessed for each complex in its minimum energy conformation.

Analysis of the data allows several trends to be identified. Among complexes containing the Fp [$CpFe(CO)_2$] fragment, significant differences emphasize the importance not only of σ and π covalent interactions but also of ionic contributions to the Fe−B bond. In all cases (except for the BPh_2 complex, **5**) electrostatic terms represent a contribution to the overall attractive interaction roughly equal to half that of covalent terms. This contrasts with the situation in iron borylene complexes ($RBFe(CO)_4$; R = Cp Me, Ph, $N(SiH_3)_2$) in which ionic terms (arising mainly from attraction between the negative electronic charge of the σ donor electron pair

at boron and the positively charged iron nucleus) are calculated to represent ca. 60% of the total attractive interaction between RB and $Fe(CO)_4$ fragments.[8d] In keeping with the results found for group 13 diyl systems, however, we find that weaker π donor boryl substituents enhance the ionic character of the M−B bond (e.g. $\Delta E_{elstat}/\Delta E_{orb} = 0.57$ for BH_2 complex **10**, 0.49 for BF_2 complex **12**). Furthermore, the degree of ionic character is consistently higher for phosphine-substituted systems than for their carbonyl analogues (e.g. **9**, **16**, **17**, **18** vs **2**, **10**, **12**, **13**, respectively). Finally, it should be noted that the electrostatic contribution for all of the (neutral) boryl complexes is shown to be significantly less than for the analogous cationic alkylidene systems.

In general, the relative contributions of σ and π symmetry covalent interactions to the M−B bond reflect the expected trends in σ donor/π acceptor properties of the boryl ligand and in the electronic properties of ancilliary ligands coordinated to the metal center. Comparison of the BH_2, BF_2, and BCl_2 derivatives **10**, **12**, and **13**, for example, reveals that the longest Fe−B bond and smallest π contribution is found for the BF_2 complex, consistent with the weaker σ donor and weaker π acceptor properties expected for the BF_2 ligand.[26] That the chloroboryl (X = Cl) and hydridoboryl (X = H) BX_2 ligands are considerably better π acceptors than BF_2 is reflected in the greater π contributions to the Fe−B bond for complexes **10** and **13**. Of the two complexes **10** and **13**, BH_2 would be expected to be not only a better π acceptor than BCl_2 but also a better σ donor. Hence, although the calculations for these two complexes reveal similar *percentage* contributions to the covalent bonding from σ and π symmetry interactions, the magnitude of the overall orbital contribution ($\Delta E_{orb} = -239.6$ kcal mol^{-1}) is ca. 13 kcal mol^{-1} higher in the case of **10**. The presence of a significant π contribution to bonding for osmium complexes of the BH_2 ligand has been predicted recently by Frenking.[7]

The strong π acceptor nature of BH_2 and BCl_2 ligands (and also of the bis(pentafluorophenyl)boryl ligand found in **8**) is also reflected in larger π contributions to the Fe−B bond than are found for catechol-based boryl ligands (e.g. in **1** and **14**) or for the asymmetric amidochloroboryl ligand found in complex **6**. The only significant exception to these trends is complex **5**, containing the BPh_2 ligand. The longer, weaker bond found by our calculations and a π contribution smaller than might have been expected for such a π acidic ligand can, however, almost certainly be attributed to its greater steric demands. Such an explanation has previously been advanced by Hartwig and co-workers to explain the results of structural studies of $CpFe(CO)_2Bcat$ and $CpFe(CO)_2BPh_2$.[3a] Finally, quaternization of the boron center, as in **7**, leads to the expected longer and weaker Fe−B bond (as found experimentally[6f]) and essentially negligible π interaction.

Variation in the metal−ligand fragment can also have a significant impact on the nature of the M−B bond.

(26) Crystallographically characterized complexes containing the BF_2 ligand have recently been reported: (a) Kerr, A.; Marder, T. B.; Norman, N. C.; Orpen, A. G.; Quayle, M. J.; Rice, C. R.; Timms, P. L.; Whittel, G. R. *Chem. Commun.* **1998**, 319. (b) Lu, N.; Norman, N. C.; Orpen, A. G.; Quayle, M. J.; Timms, P. L.; Whittell, G. R. *J. Chem. Soc., Dalton Trans.* **2000**, 4032.

Table 5. NBO Analysis of Complexes 2, 10, and 12

	Fe				B		charge	
compd	%	% s	% p	% d	% s	% p	Fe	B
2	60.0	30.8	0.0	69.1	43.5	56.5	−0.3076	0.9644
10	62.7	30.5	0.1	69.4	30.2	69.8	−0.2717	0.2724
12	58.0	30.3	0.1	69.6	63.7	36.3	−0.2841	1.1160

For example, coordination at the metal center of model phosphine ligands rather than CO (e.g. PH_3 in complexes **16**−**18**) leads to increased Fe−B BDEs and bond orders, consistent with the weaker π acceptor nature of the ancilliary PH_3 ligand.. Comparison of the isoelectronic iron and cobalt complexes $[CpFe(CO)_2BO_2C_2H_2]$ (**2**) and $[CpCo(CO)_2BO_2C_2H_2]^+$ (**19**) reveals a stronger, shorter bond in the case of **19**. Enhanced σ donation from the boryl ligand to the cobalt center in cationic **19** compensates for the most part for drastically reduced π contribution to bonding (4.2% for **19** vs 12.3% for **2**); in addition the electrostatic component ΔE_{elstat} is significantly enhanced. Finally, comparison of complexes **2** and **20** reveals a greater π contribution to the M−B bond in the case of ruthenium boryls,[3e,6d,e,15e] in keeping with the less contracted nature of the valence d orbitals.

By means of comparison, analysis of the metal boron interaction in complexes **2**, **10**, and **12** has been carried out by NBO methods (Table 5). In keeping with the analysis of Frenking et al.,[7] this reveals that the iron−boron bond is polarized markedly toward iron (the iron part of the bond orbital representing ca. 60%). For the model catecholboryl complex **2** the approximate hybridization schemes are between sd^3 and sd^2 (for Fe) and between sp^2 and sp (for B). Of particular note is the significant increase in p character at the boron end of the iron−boron bond for the strongly π acidic BH_2 ligand (in **10**) and the signifigantly reduced p character at boron for the weakly π acidic BF_2 ligand (in **12**). Such a finding is consistent with the relative importance of the π contribution to the covalent interaction found in our preceding analysis (i.e. the calculated σ:π ratio for $BO_2C_2H_2$, BH_2, and BF_2 complexes) and also with results reported by Frenking et al. for osmium boryl complexes.[7] NBO calculated charges for complexes **2**, **10**, and **12** reveal an $Fe^{\delta-}-B^{\delta+}$ spread of charge which is consistent with the known reactivity of similar complexes.[3a] In common with a recent analysis of bonding in iron borylene complexes, we find no direct correlation between NBO charges at iron and boron and the electrostatic contribution to the interaction energy (ΔE_{elstat}).[8d] Frenking and co-workers have ascribed this observation to the fact that the charge attraction is principally derived from the interaction between the negatively charged lone pair at boron and the positively charged iron nucleus and *not* between overall positively charged boron and negatively charged iron.[8d] As such, the overall atomic partial charges are not directly related to ΔE_{elstat}.

Conclusions

The results outlined above indicate that density functional theory can be used to good effect, not only to reproduce experimentally observed structural parameters for cyclopentadienyl transition metal boryl complexes but also to provide insight into the nature of the metal−boron bond. The energy partitioning analysis

allows the evaluation of the ionic/covalent character of the bond, and the decomposition of bond order analysis has enabled the relative contributions from σ and π symmetry covalent interactions to be quantified. The main conclusions reached on the basis of this analysis are as follows. (i) Covalent terms are roughly twice as important to the overall instantaneous metal−boryl interaction than are ionic terms, with the relative importance of electrostatics increasing for weaker π donor boryl substituents (X) and weaker π acceptor ancilliary ligands at the metal. (ii) The relative contributions from σ and π symmetry covalent interactions emphasize the description of boryl ligands as extremely good σ donors but relatively poor π acceptors. The high energy of the vacant boryl-centered π orbital ensures that even in favorable cases the π contribution to the covalent bonding interaction does not exceed 15−20% (15.8, 17.8, and 18.0% for $CpFe(CO)_2BH_2$ (**10**), $CpFe(CO)_2BCl_2$ (**13**), and $CpFe(CO)_2B(C_6F_5)_2$ (**8**), respectively).

Computational Methodology

Gradient-corrected DFT calculations were carried out using the ADF2000.01 code,[27] with functionals for exchange and correlation due to Becke[28] and Lee, Yang, and Parr,[29] respectively. A basis set constructed from Slater type orbitals with triple-ζ valence shell and a single polarization function per atom was used for all calculations (ADF IV). The level of frozen core approximation for B, C, N, O, and F was the 1s orbital and for P, Cl, Fe, and Co was the 2p orbital; an effective core potential was employed for Ru. All structures, unless otherwise stated, were fully optimized with no symmetry restrictions. Convergence was accepted when the following limits were met: (i) energy change on next step $<1 \times 10^{-3}$ hartree, (ii) gradient $<1 \times 10^{-3}$ hartree Å^{-1}, and (iii) uncertainty in Cartesian coordinates $<1 \times 10^{-2}$ Å. The multiplicity of each structure was determined by using unrestricted calculations with spin states set to reasonable alternatives to determine the lowest energy configuration which conformed to the aufbau principle. A scalar relativistic (SR) zero-order regular approximation (ZORA) was used for all compounds containing ruthenium within this study.[30]

To picture the distribution of charge in the M−B bond, density difference plots were generated by subtracting the superposition of noninteracting atomic densities (at the calculated molecular geometry) from the calculated molecular density. This is easily achieved within ADF, since the former charge distribution is the starting point for the self-consistent field portion of the calculation.

The bond dissociation energy for given M−B bonds was calculated by estimating the energy change associated with the homolytic bond cleavage reaction:

$$[(C_5R_5)ML_2(BX_2)]^{n+} \rightarrow [(C_5R_5)ML_2]^{n+} + BX_2$$

The structures of the products from this reaction were independently optimized to allow for the inclusion of any molecular relaxation. Due to the large number of structures considered, zero-point energy contributions for these bond energies were not calculated. The effect of basis set superposition error (BSSE) on the bond dissociation energy for compound **1** was calculated using the counterpoise method to be of the order of 1.7 kcal mol^{-1}, a value comparable to that found for metal−carbonyl and metal−metal bonds using similar basis sets (1.5−2 kcal mol^{-1}).[31] Since this is only 2−3% of the total BDE, and BSSE is expected to introduce a systematic error, we did not calculate its effect on other complexes. The small magnitude of the BSSE suggests that the basis set being used is of high quality, in agreement with our conclusions based on Fe−B bond length as a function of basis set.

The electrostatic contribution to the bond was calculated by a further single-point calculation in which the two parts of the complex were treated as ADF fragments. Since ADF decomposes the interaction energy between fragments into electrostatic, Pauli repulsion, and orbital components,[32] this calculation gave the electrostatic contribution to bonding directly. This partition of the energy takes into account the anisotropy of the charge density, which is particularly important in the bonding region between a Lewis acid and the donor atom of a base, since the charge density on the base will be strongly polarized by the presence of the acid, as discussed in ref 8d.

Since the computational cost of DFT calculations increases with the number of electrons in the optimized system, we have carried out calculations using a simplified (or "cut down") version of the widely used catecholboryl ligand. Here the benzo group (*o*-C_6H_4) is replaced by a single cis substituted C═C bond (resulting in a $-BO_2C_2H_2$ ligand rather than $BO_2C_6H_4$) in order to reduce the size of the system while maintaining the five-membered chelate structure.

To study the effect of the variation of level of theory and basis set on the Fe−B bond length, calculations were also performed using the Gaussian 98 program.[33] Full geometry optimization was carried out with the use of the BLYP[28,29] and B3LYP[34] density functional level of theory combined with several basis sets: STO-3G,[35] LANL2DZ,[36] and 6-311G(d), 6-31+G(d), and 6-311++G(d)[37] were incorporated on all atoms.

To calculate the degree of σ and π bonding between the metal center and boron atom, the optimized structures were reoriented so that the bond was aligned with the *z* axis. A bonding analysis was then carried out following the approach discussed below to give contributions to the bonding density segregated according to the symmetry of the atomic orbitals involved.

(27) (a) Baerends, E. J.; Ellis, D. E.; Ros, P. *Chem. Phys.* **1973**, *2*, 41. (b) Versluis, L.; Ziegler, T. *J. Chem. Phys.* **1988**, *88*, 322. (c) te Velde, G.; Baerends, E. J. *J. Comput. Phys.* **1992**, *99*, 84. (d) Fonseca Guerra, C.; Snijders, J. G.; te Velde, G.; Baerends, E. J. *Theor. Chem. Acta* **1998**, *99*, 391.

(28) Becke, A. D. *Phys. Rev. A* **1988**, *38*, 3098.

(29) Lee, C.; Wang, W.; Parr, R. G. *Phys. Rev. B* **1988**, *37*, 785.

(30) (a) Snijders, J. G.; Baerends, E. J.; Ros, P. *Mol. Phys.* **1979**, *38*, 1909. (b) Ziegler, T.; Tschinke, V.; Baerends, E. J.; Snijders, J. G.; Ravenek, W. *J. Phys. Chem.* **1989**, *93*, 3056. (c) van Lenthe, E.; Baerends, E. J.; Snijders, J. G. *J. Chem. Phys.* **1993**, *99*, 4597.

(31) Rosa, A.; Ehlers, A. W.; Baerends, E. J.; Snijders, J. G.; te Velde, G. *J. Phys. Chem.* **1996**, *100*, 5690.

(32) Ziegler, T.; Rauk, A. *Inorg. Chem.* **1979**, *18*, 1755.

(33) Frisch, M. J.; Trucks, G. W.; Schlegel, H. B.; Scuseria, G. E.; Robb, M. A.; Cheeseman, J. R.; Zakrzewski, V. G.; Montgomery, J. A., Jr.; Stratmann, R. E.; Burant, J. C.; Dapprich, S.; Millam, J. M.; Daniels, A. D.; Kudin, K. N.; Strain, M. C.; Farkas, O.; Tomasi, J.; Barone, V.; Cossi, M.; Cammi, R.; Mennucci, B.; Pomelli, C.; Adamo, C.; Clifford, S.; Ochterski, J.; Petersson, G. A.; Ayala, P. Y.; Cui, Q.; Morokuma, K.; Malick, D. K.; Rabuck, A. D.; Raghavachari, K.; Foresman, J. B.; Cioslowski, J.; Ortiz, J. V.; Stefanov, B. B.; Liu, G.; Liashenko, A.; Piskorz, P.; Komaromi, I.; Gomperts, R.; Martin, R. L.; Fox, D. J.; Keith, T.; Al-Laham, M. A.; Peng, C. Y.; Nanayakkara, A.; Gonzalez, C.; Challacombe, M.; Gill, P. M. W.; Johnson, B. G.; Chen, W.; Wong, M. W.; Andres, J. L.; Head-Gordon, M.; Replogle, E. S.; Pople, J. A. *Gaussian 98*, revision A.9; Gaussian, Inc.: Pittsburgh, PA, 1998.

(34) Becke, A. D. *J. Chem. Phys.* **1993**, *98*, 5648.

(35) (a) Hehre, W. J.; Stewart, R. F.; Pople, J. A. *J. Chem. Phys.* **1969**, *51*, 2657. (b) Collins, J. B.; Schleyer, P. v. R.; Binkley, J. S.; Pople, J. A. *J. Chem. Phys.* **1976**, *64*, 5142.

(36) (a) Dunning, T. H. Jr.; Hay, P. J. In *Modern Theoretical Chemistry*; Schaefer, H. F., III, Ed.; Plenum: New York, 1976; pp 1−28. (b) Hay, P. J.; Wadt, W. R. *J. Chem. Phys.* **1985**, *82*, 270. (c) Wadt, W. R.; Hay, P. J. *J. Chem. Phys.* **1985**, *82*, 284. (d) Hay, P. J.; Wadt, W. R. *J. Chem. Phys.* **1985**, *82*, 299.

(37) (a) Krishnan, R.; Binkley, J. S.; Seeger, R.; Pople, J. A. *J. Chem. Phys.* **1980**, *72*, 650. (b) Hay, P. J. *J. Chem. Phys.* **1970**, *52*, 1033. (c) Curtiss, L. A.; McGrath, M. P.; Blaudeau, J.-P.; Davis, N. E.; Binning, R. C., Jr.; Radmon, L. *J. Chem. Phys.* **1995**, *103*, 6104.

The one-electron wave functions, ψ_i, used to represent the density in these DFT calculations are constructed in the usual manner as a linear combination of atomic basis functions, ϕ:

$$\psi_i = \sum_k^M c_{ik}\phi_k \tag{1}$$

where c_{ik} is the coefficient of the kth basis function in the ith molecular orbital and there are a total of M basis functions. The density, ρ, is then given by summation over the occupied orbitals of the one-electron densities:

$$\rho = 2\sum_i^{N/2}\sum_l^M c_{il}\phi_l \sum_k^M c_{ik}\phi_k = 2\sum_l^M\sum_k^M \phi_l\phi_k \sum_i^{N/2} c_{il}c_{ik} \tag{2}$$

where N is the total number of electrons and we only consider the restricted spin-paired situation for simplicity; extension to the spin-unrestricted case is straightforward. The rearranged form of the density expression allows the calculation to be performed via the definition of two square matrixes with the dimension M. The first is usually referred to as the density matrix, **P**, and its components depend only on the calculated coefficients:

$$P_{lk} = \sum_i^{N/2} c_{il}c_{ik} \tag{3}$$

The second, the overlap matrix, **S**, depends on the basis set and the geometry of the molecule through the integrals:

$$S_{lk} = \int \phi_l\phi_k \, d\tau \tag{4}$$

which are formally over all space. The density can then be represented as a matrix multiplication:

$$\rho = 2\sum_l^M\sum_k^M S_{lk}P_{kl} \tag{5}$$

Since the basis set consists of atom-centered functions, **P** and **S** will contain some contributions which are wholly centered on a given atom and some which are due to the overlap of basis functions on pairs of atoms. The latter contribution is related to the bonding between atoms, and the most straightforward way to address the character of bonding is to examine this portion in isolation. By identifying the basis functions centered on a pair of atoms, e.g. A and B, we can identify the bonding density, ρ_{AB}, by summing only the relevant contributions in eq 6:

$$\rho_{AB} = 2\sum_{l\in A}\sum_{k\in B} S_{lk}P_{kl} \tag{6}$$

This is the bonding density as defined by Mulliken.[38] To differentiate π and σ contributions to the bonding density, we simply align the bond of interest with the z direction and separate the basis functions according to their symmetry; e.g., p_z is of σ type and p_x and p_y are of π type. Equation 6 can then be further subdivided:

$$\rho_{AB} = 2\sum_{l\in A}^{\sigma}\sum_{k\in B}^{\sigma} S_{lk}P_{kl} + 2\sum_{l\in A}^{\pi}\sum_{k\in B}^{\pi} S_{lk}P_{kl} + 2\sum_{l\in A}^{\delta}\sum_{k\in B}^{\delta} S_{lk}P_{kl} + \ldots \tag{7}$$

where the symmetry labels on the summations indicate the basis function symmetry to be considered. In the program developed for this work, the molecular orbital coefficients and overlap matrix elements are read from the ADF output file and the density associated with the Fe−B bond is separated into σ and π contributions corresponding to the terms in eq 7. Both the metal- and boron-centered basis functions are assigned a symmetry label, σ, π, or δ, and the corresponding density is accumulated only from orbitals with matching symmetry labels. In addition, contributions from differing orbital symmetries (e.g., σ with π) are evaluated to check for mixing between bonding types, however the calculated mixing contribution was always found to be zero to the four-decimal-place accuracy used for the orbital coefficients in the ADF output file.

This decomposition of the molecular orbital representation of the density to give bonding density is not unique, and so to ensure the reliability of our analysis, we also consider a bonding density analysis proposed by Mayer.[39] In the Mayer analysis the product of the density and overlap matrixes is first calculated and then the elements of this product matrix are selected according to the basis functions belonging to the atoms of interest. Again we further partition the matrix in terms of π and σ symmetry:

$${\rho_{AB}}^M = 2\sum_{l\in A}^{\sigma}\sum_{k\in B}^{\sigma} (PS)_{kl} + 2\sum_{l\in A}^{\pi}\sum_{k\in B}^{\pi} (PS)_{kl} \tag{8}$$

As part of this work, the application of eqs 7 and 8 to the data provided by an ADF output was automated by the development of a dedicated program. The coding was tested by calculation of the Mulliken atomic densities which are output by ADF and by analysis of simple test cases such as ethane, ethene, ethyne, etc. (these analyses are included in the Supporting Information). The Mayer bond order calculation was tested by comparing values obtained from our analysis of ADF outputs and those generated at a similar basis set level by the MSI code DMOL^3.[40] The results of decomposition into σ and π contributions from Mulliken and Mayer approaches consistently showed the same trends, and so only the former is reported in the main text.

Natural atomic orbitals[41] are generated by diagonalizing the block diagonal portions of the density matrix concerned with each atom in the system. This allows a localized picture of the atomic orbitals that are involved in bonding to be generated. Natural bond orbitals are then derived from the overlap elements of the new density matrix. This procedure leads to atomic charges and overlap populations which converge with increasing basis set size, in contrast to earlier schemes such as Mulliken analysis. NBO calculations were carried out at the B3LYP/LANL2DZ level of theory.

Acknowledgment. The calculations presented in this paper were carried out, in part, using 'Glyndwr,' a Silicon Graphics multiprocessor Origin 2000 machine at the Department of Chemistry, Cardiff University. This facility was purchased with support from the EPSRC, Synetix, and OCF.

Supporting Information Available: Listings of bond orders and σ and π contributions to bonding density for the test molecules ethane, ethene, ethyne, carbon monoxide, and dinitrogen, electron density difference maps for compounds **2** and **11**, pictorial representations of Kohn−Sham orbitals for complexes **2** and **9**−**11** relevant to the discussion in the text, and listings of atomic orbital contributions to relevant Kohn−Sham orbitals for **2** and **9**−**11**. This material is available free of charge via the Internet at http://pubs.acs.org.

OM0105122

(38) Mulliken, R. S. *J. Chem. Phys.* **1955**, *23*, 1833.

(39) Mayer, I. *Int. J. Quantum Chem.* **1986**, *29*, 477.

(40) DMOL^3; Biosym/MSI, San Diego, CA, 1996.

(41) Reed, A. E.; Curtiss, L. A.; Weinholt, F. *Chem. Rev.* **1988**, *88*, 899.